Lea, C. H., Rhodes, D. N., & Stell, R. D. (1955) *Biochem. J. 60*, 353–363.
Nomura, T., & Kurihara, K. (1987) *Biochemistry* (preceding paper in this issue).
Pelosi, P., Baldaccini, N. E., & Pisanelli, A. M. (1982) *Biochem. J. 201*, 245–248.
Pevsner, J., Trifiletti, R. R., Strittmatter, S. M., & Snyder, S. H. (1985) *Proc. Natl. Acad. Sci. U.S.A. 82*, 3050–3054.
Pevsner, J., Sklar, P. B., & Snyder, S. H. (1986) *Proc. Natl. Acad. Sci. U.S.A. 83*, 4942–4946.
Price, S. (1981) in *Biochemistry of Taste and Olfaction* (Cagan, R. H., & Kare, M. R., Eds.) pp 69–84, Academic, New York.
Price, S. (1984) *Chem. Senses 8*, 341–354.
Sicard, G. (1985) *Brain Res. 326*, 203–212.
Sicard, G., & Holley, A. (1984) *Brain Res. 292*, 283–296.
Suzuki, N. (1977) in *Food Intake and Chemical Senses* (Katsuki, Y., Sato, M., Takagi, S. F., & Oomura, Y., Eds.) pp 13–22, University of Tokyo Press, Tokyo.
Trotier, D., & MacLeod, P. (1983) *Brain Res. 268*, 225–237.

Time-Resolved Tryptophan Fluorescence Anisotropy Investigation of Bacteriophage M13 Coat Protein in Micelles and Mixed Bilayers†

Klaas P. Datema,*,‡ Antonie J. W. G. Visser,§ Arie van Hoek,‡ Cor J. A. M. Wolfs,‡ Ruud B. Spruijt,‡ and Marcus A. Hemminga‡

Departments of Molecular Physics and Biochemistry, Agricultural University, Wageningen, The Netherlands

Received February 11, 1987; Revised Manuscript Received May 4, 1987

ABSTRACT: Coat protein of bacteriophage M13 is examined in micelles and vesicles by time-resolved tryptophan fluorescence and anisotropy decay measurements and circular dichroism experiments. Circular dichroism indicates that the coat protein has α-helix (60%) and β-structure (28%) in 700 mM sodium dodecyl sulfate micelles and predominantly β-structure (94%) in mixed dimyristoylphosphatidylcholine/dimyristoylphosphatidic acid (80/20 w/w) small unilamellar vesicles. The fluorescence decay at 344 nm of the single tryptophan in the coat protein after excitation at 295 or 300 nm is a triple exponential. In the micelles the anisotropy decay is a double exponential. A short, temperature-independent correlation time of 0.5 ± 0.2 ns reflects a rapid depolarization process within the coat protein. The overall rotation of the coat protein–detergent complex is observed in the decay as a longer correlation time of 9.8 ± 0.5 ns (at 20 °C) and has a temperature dependence that satisfies the Stokes–Einstein relation. In vesicles at all lipid to protein molar ratios in the range from 20 to 410, the calculated order parameter is constant with a value of 0.7 ± 0.1 from 10 to 40 °C, although the lipids undergo the gel to liquid-crystalline phase transition. The longer correlation time decreases gradually on increasing temperature. This effect probably arises from an increasing segmental mobility within the coat protein. The results are consistent with a model in which the coat protein has a β-structure and the tryptophan indole rings do not experience the motion of the lipids in the bilayer because of protein–protein aggregation.

The interaction of membrane proteins with lipids has received considerable attention in the last decade. The interest in understanding this interaction arises from the notion that lipid composition and dynamics in membranes affect the properties of its proteins. A variety of biophysical techniques has already been applied to membrane proteins reconstituted in model membranes [for a survey, see Watts and De Pont (1985)]. Model membranes can easily be prepared and are free of the complexity of the natural membrane. In particular, time-resolved fluorescence anisotropy measurements [for a review, see Cundall and Dale (1983) and Beechem and Brand (1985)] and nuclear magnetic resonance (NMR)[1] provide complementary information about motion and order of lipids in bilayer systems [for a comparison, see Wolber and Hudson (1982) and Devaux and Seigneuret (1985)].

The objective of our research is to study the infection mechanism of nonenveloped viruses, like bacteriophage M13 (Hemminga, 1987) and plant viruses (Hemminga et al., 1985), at a molecular level. A suitable system to study the interaction of viral coat proteins with membranes is the M13–*Escherichia coli* system.

The major (gene 8 product) M13 coat protein is present in the long rodlike virus particle in numerous copies and functions as protection for its single-strand DNA. The virus enters *E. coli* by leaving the coat proteins in the cytoplasmic membrane (Marvin & Wachtel, 1975). After infection and DNA duplication, the newly synthesized procoats, a precursor form of the coat protein with a typical bacterial amino-terminal leader

† This research was supported by the Netherlands Foundation of Biophysics with financial aid from the Netherlands Organization for the Advancement of Pure Research (ZWO). Preliminary results of this work were presented at the 13th International Congress of Biochemistry, Amsterdam, The Netherlands, 1985.

* Author to whom correspondence should be addressed.
‡ Department of Molecular Physics.
§ Department of Biochemistry.

[1] Abbreviations: NMR, nuclear magnetic resonance; CD, circular dichroism; DMPC, 1,2-dimyristoyl-*sn*-glycero-3-phosphocholine; DMPA, 1,2-dimyristoyl-*sn*-glycero-3-phosphatidic acid; SUVs, small unilamellar vesicles; SDS, sodium dodecyl sulfate; L/P ratio, phospholipid to coat protein molar ratio; cmc, critical micelle concentration; OD_{280nm}, optical density at 280 nm; S, order parameter; $r(0)$, initial anisotropy; $r(\infty)$, residual anisotropy; Tris-HCl, tris(hydroxymethyl)aminomethane hydrochloride; EDTA, ethylenediaminetetraacetic acid.

0006-2960/87/0426-6145$01.50/0

peptide of 23 residues, also assemble in this membrane. After penetration of the N-terminus of the procoat through the membrane, the procoat is cleaved to mature coat protein by a leader peptidase (Geller & Wickner, 1985). Both progeny and parental coat protein are used for the membrane-bound assembly of new M13 particles (Wickner, 1976). The viral DNA is complexed with these coat proteins without lysis of the host cell.

The coat protein consists of 50 amino acid residues (M_r 5240): a basic C-terminus, a hydrophobic central core of 19 amino acid residues, and an acidic N-terminus (Van Asbeck et al., 1969; Nakashima & Konigsberg, 1974). It contains a single tryptophan residue located at the 26th position, i.e., in the hydrophobic region. The tryptophan can be used as an intrinsic fluorescent marker.

Time-resolved fluorescence anisotropy analysis of fluorophores in membranes [for a theoretical description, see, for example, Kinosita et al. (1977, 1982), Zannoni et al. (1983), Szabo (1984), and Van der Meer et al. (1984)] has several features that make the technique particularly attractive for studying the M13 coat protein in model membranes. First, the time-dependent anisotropy provides a direct, real-time measurement of the reorientational dynamics of the coat protein in the (sub)nanosecond time range. The measurable range is limited by the average fluorescence lifetime characterizing the tryptophan. Second, in time-resolved fluorescence anisotropy analysis motional rates and molecular order manifest themselves separately, which is advantageous for bilayer studies.

We have reconstituted the coat protein of M13 in micelles and mixed SUVs. Time-resolved fluorescence and fluorescence anisotropy measurements of the single tryptophan residue in the coat protein were carried out at various temperatures and protein contents. In addition, CD spectra were taken of the coat protein in these micelles and bilayers to determine the secondary structure of the coat protein. Time-resolved fluorescence and fluorescence anisotropies were analyzed in terms of multiexponential functions, giving information about dynamics of the coat protein tryptophan and the structure of its environs in these systems. In SUVs an additional residual anisotropy in present, which is directly related to the order of the coat protein tryptophan. The temperature dependence of the correlation times and of the order of the coat protein in the membrane was determined in the range in which the lipid bilayer undergoes the gel to liquid-crystalline phase transition.

Materials and Methods

Materials. DMPC (1,2-dimyristoyl-*sn*-glycero-3-phosphocholine, 99% purity) and DMPA (1,2-dimyristoyl-*sn*-glycero-3-phosphatidic acid, 98% purity) were obtained from Sigma Chemical Co. and used without further purification. M13 bacteriophage was purified as described by Garssen et al. (1977). The major (gene 8 product) coat protein of M13 was isolated by the method of Knippers and Hoffmann-Berling (1966).

Sample Preparation. Micelles were prepared by dissolving coat protein in 0.8, 4, 100, or 700 mM SDS–10 mM potassium phosphate, pH 5.0. A clear, micellar solution was obtained by vortexing and heating the sample to 55 °C. The samples were diluted with the same buffers to $OD_{280nm} = 0.1$.

Vesicles were prepared by cholate dialysis, as described by Hagen et al. (1978) with a few modifications. Stock suspensions of DMPC and DMPA vesicles (both 50 mg/mL) and coat protein (8 mg/mL) in 5.0 mM Tris-HCl buffer, pH 8.0, with 2 wt% sodium cholate, 8.0 M urea, 0.1 mM EDTA, and 20 mM ammonium sulfate were used; 0.16 mL of DMPC stock suspension, 0.04 mL of DMPA stock suspension, and 0.500, 0.250, 0.125, 0.063, 0.031, 0.016, or 0 mL of coat protein stock solution were coadded with 0.300, 0.550, 0.675, 0.737, 0.769, 0.784, or 0.800 mL of the same buffer, respectively. Clear and homogeneous suspensions were obtained by vortexing and heating the samples to 55 °C. Subsequently, the suspensions were dialyzed at 4 °C against 4 times 1.5 L of 10 mM Tris-HCl, pH 8.0, 0.2 mM EDTA, and 10% (v/v) methanol during 48 h with changes at 12, 24, and 36 h. In the last dialysis step no methanol was added to the buffer. This results in opalescent dispersions of unilamellar vesicles. All the samples were sonicated under nitrogen with a Branson cell disruptor B30 [duty cycle: 90%, power setting 4 (maximum 350 W at setting 10)] to obtain SUVs. The SUV suspensions were centrifuged (8800*g*, 10 min) to precipitate unincorporated, water-insoluble coat protein. At this point, aliquots of the samples were taken to determine the protein and phospholipid concentration (Bartlett, 1959; Peterson, 1977), from which the L/P ratio was calculated. This procedure results in samples of L/P ratios of 20, 30, 70, 140, 210, 410, or ∞, respectively. The error in these ratios was less than 10%. The samples were homogeneous as tested by sucrose gradient centrifugation. Before measurement, the samples were diluted to $OD_{280nm} = 0.1$.

Methods. CD spectra were recorded at room temperature on a Jobin-Yvon Auto-Dichrograph Mark V in the wavelength range 250–190 nm. A sample cell of 1-mm path length was used. The spectra are the average of four scans taken from the same sample. To determine the secondary structure, the CD spectra were fitted to reference spectra of Greenfield and Fasman (1969) by a least-squares fitting procedure with spectral points in the 250–190-nm range with 5-nm steps. The basis for this analysis has been described (Cantor & Schimmel, 1980).

The experimental setup for the time-resolved fluorescence measurements has been described previously (Van Hoek et al., 1983; Van Hoek & Visser, 1985; Visser et al., 1985). The excitation wavelengths were 295 and 300 nm. The emission wavelength was selected with an interference filter transmitting at 344 nm with a 10-nm band-pass. Fluorescence was detected by time-correlated single-photon counting (O'Connor & Phillips, 1984).

The total fluorescence decay is determined from the measured polarized fluorescence components parallel, $I_{\parallel}$, and perpendicular, $I_{\perp}$ to the electric vector of the excitation as

$$S(t) = I_{\parallel}(t) + 2I_{\perp}(t) \tag{1}$$

in which $S(t)$ is the convolution product of the (unconvoluted) total fluorescence $s(t)$ and the excitation pulse response $P(t)$. The data were analyzed as a sum of three exponentials, i.e.

$$s(t) = \sum_{i=1}^{3} \alpha_i \exp(-t/\tau_i) \tag{2}$$

in which τ_i is the fluorescence lifetime with a preexponential factor α_i indicating the relative contribution of τ_i to the initial intensity of the total decay. The experimental data were corrected for background fluorescence measured for identical vesicles without coat protein (in all cases less than 10% of the fluorescence of the sample with coat protein). From these data the lifetimes and relative contributions to the total decay are obtained by a nonlinear least-squares fitting procedure (Vos et al., 1987).

The fluorescence anisotropy $r(t)$ is given by

$$r(t) = [i_{\parallel}(t) - i_{\perp}(t)]/[i_{\parallel}(t) + 2i_{\perp}(t)] \tag{3}$$

Table I: Fluorescence Decay Parameters (344 nm) of the Single Tryptophan of Bacteriophage M13 Coat Protein in SDS Micelles for Excitation at 295 nm[a]

SDS (mM)	T (°C)	$\alpha_1 \pm 0.05$	$\tau_1 \pm 0.1$ (ns)	$\alpha_2 \pm 0.05$	$\tau_2 \pm 0.1$ (ns)	$\alpha_3 \pm 0.05$	$\tau_3 \pm 0.1$ (ns)	$\langle\tau\rangle$ (ns)
0.8	20	0.30	1.2	0.62	3.7	0.08	7.5	4.1
4	20	0.18	0.9	0.52	3.1	0.30	5.8	4.4
100	20	0.23	0.3	0.30	2.3	0.46	5.5	4.7
700	20	0.22	0.3	0.29	2.5	0.49	5.7	5.0
700	25	0.23	0.3	0.29	2.5	0.47	5.6	4.8
700	30	0.27	0.3	0.28	2.3	0.46	5.3	4.6
700	35	0.19	0.3	0.27	2.0	0.54	4.9	4.4
700	40	0.17	0.3	0.27	1.8	0.56	4.6	4.1

[a] $\langle\tau\rangle = \sum_{i=1}^{3}\alpha_i\tau_i^2/\sum_{i=1}^{3}\alpha_i\tau_i$.

Table II: Anisotropy Decay Parameters (344 nm) of the Single Tryptophan of Bacteriophage M13 Coat Protein in SDS Micelles for Excitation at 295 nm[a]

SDS (mM)	T (°C)	$\beta_1 \pm 0.01$	$\phi_2 \pm 0.5$ (ns)	$\beta_2 \pm 0.01$	$\phi_2 \pm 0.5$ (ns)	$r(0) \pm 0.02$	$V \times 10^{-3}$ (cm^3)
0.8	20	0.06	0.5	0.09	16.2	0.15	
4	20	0.07	0.5	0.10	10.2	0.17	24
100	20	0.05	0.5	0.10	9.6	0.15	23
700	20	0.06	0.5	0.11	9.8	0.17	23
700	25	0.06	0.5	0.11	9.1	0.16	25
700	30	0.04	0.5	0.11	7.6	0.15	24
700	35	0.05	0.5	0.10	6.9	0.15	25
700	40	0.05	0.5	0.09	6.1	0.14	24

[a] β_i is the contribution to the initial anisotropy, $r(0)$, of the depolarization mechanism characterized by ϕ_i; V, the volume of the protein–micelle complex, was calculated with the Stokes–Einstein relation for spherical rotation; $\phi_2 = \eta V/RT$ in which η is the viscosity of water, T is the temperature, and R is the gas constant.

in which $i_\parallel(t)$ and $i_\perp(t)$ are the (deconvoluted) parallel and perpendicular polarized components derived from the experimental $I_\parallel(t)$ and $I_\perp(t)$components. $r(t)$ is obtained by fitting the experimental $I_\parallel(t)$ and $I_\perp(t)$ decays directly to the anisotropy-containing expressions for these two fluorescence components with the use of one set of parameters (Gilbert, 1983; Cross & Fleming, 1984) on Fortran-77 programs (Vos et al., 1987). The model for anisotropy decay analysis consisted of a sum of two exponentials for the coat protein in micelles and of a sum of two exponentials and a constant term for the coat protein in SUVs. In the analysis it is assumed that every lifetime component is coupled to every rotational component (Dale et al., 1977). The quality of the fit is determined by (1) visual inspection, (2) the weighted residuals, (3) the number of zero passages of the autocorrelation function (Ameloot & Hendrickx, 1982), (4) the reduced χ^2 value, (5) the Durbin–Watson parameter (O'Connor & Phillips, 1984), and (6) the standard deviations. The standard deviations of the fitted parameters are estimated from the Hessian as described by Bevington (1969), which is one of the output parameters of the Fortran-77 programs.

The orientational order parameter S for the coat protein in the bilayer is calculated from the residual, $r(\infty)$, and the initial, $r(0)$, anisotropies by

$$S = [r(\infty)/r(0)]^{1/2} \quad (4)$$

as given by Heyn (1979) and Jaehnig (1979). For $r(0)$ the average of the series of measurements at each excitation wavelength was used (Table IV).

Results

Circular Dichroism. The CD spectrum of M13 coat protein in micelles is shown in Figure 1. Analysis of the spectrum yields 60% α-helix, 28% β-structure, and 12% other structure for the coat protein in 700 mM SDS micelles. Below the cmc (which is at 3 mM; Helenius et al., 1979) at 0.8 mM SDS, 16% α-helix, 64% β-structure, and 20% other structure were determined (data not shown). The CD spectrum of M13 coat protein in mixed SUVs of DMPC/DMPA (20/80 w/w) at an L/P ratio of 25 was best simulated by 2% α-helix, 94% β-structure, and 4% other structure (Figure 1). The same CD spectra were observed for the other L/P molar ratios (data not shown).

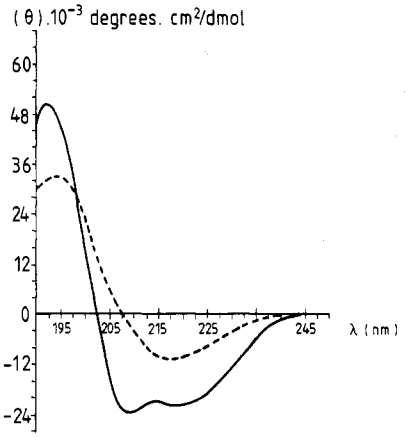

FIGURE 1: CD spectra of M13 coat protein at 20 °C in 700 mM SDS micelles (solid line) and mixed SUVs of DMPC/DMPA (80/20 w/w) at L/P ratio of 25 (dashed line). Mean residue ellipticities are shown.

Time-Resolved Fluorescence of M13 Coat Protein in Micelles. The total fluorescence decay at 344 nm of M13 coat protein in micelles after excitation at 295 nm was fitted as a triple-exponential function (an example of a triple-exponential fit, for the decay of M13 coat protein in mixed SUVs, is shown in Figure 4). The lifetimes that characterize the total fluorescence decays of the M13 coat protein–SDS complexes and their relative contributions to the total decay are listed in Table I. In 700 mM SDS the shortest lifetime, τ_1, and all the amplitudes are independent of temperature. However, τ_2 and τ_3 decrease at increasing temperature (Table I). Below the cmc (3 mM), all lifetimes increase, while α_2, and possibly α_1, increase at the expense of α_3.

The fluorescence anisotropy decay was fitted as a double-exponential function. In Figure 2 the anisotropy decay at 344 nm of M13 coat protein in 700 mM SDS micelles at 20 °C is given. The correlation times and their amplitudes are listed in Table II for various SDS concentrations and temperatures. The short correlation time, ϕ_1 (0.5 ± 0.2 ns), is independent

Table III: Fluorescence Decay Parameters (344 nm) of the Single Tryptophan of Bacteriophage M13 Coat Protein–DMPC/DMPA (80/20 w/w) SUVs at L/P Molar Ratio 70[a]

λ_{exc} (nm)	T (°C)	$\alpha_1 \pm 0.02$	$\tau_1 \pm 0.1$ (ns)	$\alpha_2 \pm 0.02$	$\tau_2 \pm 0.1$ (ns)	$\alpha_3 \pm 0.02$	$\tau_3 \pm 0.1$ (ns)	$\langle\tau\rangle$ (ns)
295	10	0.20	0.6	0.47	2.1	0.33	5.7	4.3
	15	0.26	0.8	0.42	2.2	0.33	5.5	4.2
	20	0.25	0.8	0.44	2.2	0.31	5.5	4.1
	25	0.24	0.9	0.41	2.1	0.35	5.1	3.9
	30	0.17	0.7	0.46	1.8	0.37	4.8	3.7
	35	0.13	0.6	0.49	1.7	0.38	4.7	3.6
	40	0.15	0.7	0.46	1.7	0.39	4.5	3.5
300	20	0.22	0.3	0.40	2.2	0.38	5.8	4.7
	25	0.14	0.3	0.46	2.2	0.40	5.6	4.5
	30	0.24	0.8	0.38	2.3	0.38	5.5	4.3
	35	0.26	0.8	0.40	2.4	0.34	5.5	4.2
	40	0.22	0.3	0.45	2.0	0.33	5.2	4.0

[a] $\langle\tau\rangle = \sum_{i=1}^{3}\alpha_i\tau_i^2/\sum_{i=1}^{3}\alpha_i\tau_i$.

Table IV: Anisotropy Decay Parameters (344 nm) of the Single Tryptophan of Bacteriophage M13 Coat Protein–DMPC/DMPA (80/20 w/w) SUVs at L/P Molar Ratio 70[a]

λ_{exc} (nm)	T (°C)	$\beta_1 \pm 0.01$	ϕ_1 (ns)	$\beta_2 \pm 0.01$	$\phi_2 \pm 2$ (ns)	$r(\infty) \pm 0.01$	$r(0)$	$S \pm 0.09$
295	10	0.03	0.5	0.04	10	0.09	0.16	0.75
	15	0.03	0.5	0.04	9	0.09	0.16	0.75
	20	0.03	0.5	0.04	8	0.09	0.16	0.75
	25	0.03	0.5	0.05	8	0.08	0.16	0.71
	30	0.03	0.5	0.05	6	0.08	0.16	0.71
	35	0.03	0.5	0.05	6	0.08	0.16	0.71
							0.16 ± 0.005[b]	
300	20	0.06	0.5	0.07	8	0.10	0.23	0.66
	25	0.06	0.5	0.09	7	0.09	0.24	0.60
	30	0.06	0.5	0.08	6	0.09	0.23	0.63
	35	0.06	0.5	0.08	6	0.09	0.23	0.63
	40	0.06	0.5	0.07	5	0.09	0.23	0.64
							0.23 ± 0.005[b]	

[a] β_i is the contribution to the initial anisotropy, $r(0)$, of the dipolarization mechanism characterized by ϕ_i. [b] $\langle r(0)\rangle$.

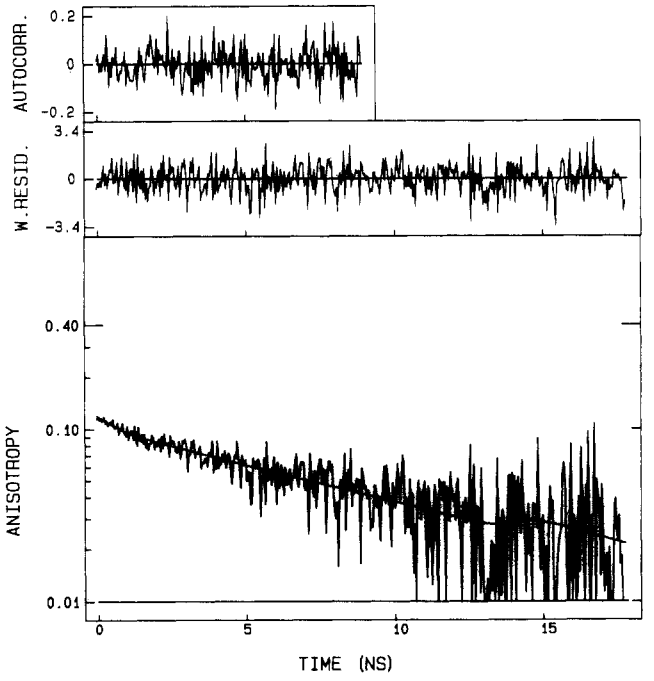

FIGURE 2: Anisotropy decay at 344 nm of the single tryptophan of bacteriophage M13 coat protein in 700 mM SDS micelles at 20 °C after excitation at 295 nm and the best computer fit. The parameters describing the best fit to the experimental decay and the estimated standard deviations are $\beta_1 = 0.06 \pm 0.014$, $\beta_2 = 0.11 \pm 0.004$, $\phi_1 = 0.50 \pm 0.21$ ns, and $\phi_2 = 9.76 \pm 0.51$ ns with the Durbin–Watson parameter = 1.95 and the number of zero passages in the parallel channel = 97 and in the perpendicular channel = 96 (429 channels, 42 ps/channel). The weighted residuals from experimental and fitted curve and the autocorrelation function are given in the top of the figure.

of both the SDS concentration and temperature. The longer correlation time, ϕ_2, depends on the SDS concentration as well as temperature. The value of ϕ_2, which is significantly longer below the cmc (3 mM), decreases as a function of temperature (Figure 3). The product $kT\phi_2/\eta$, in which η is the viscosity of pure water, is given in Table II and found to be constant within experimental error (10%).

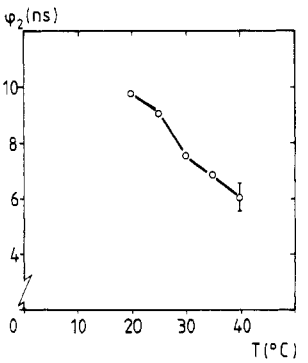

FIGURE 3: Temperature dependence of the longer correlation time, ϕ_2, of M13 coat protein in 700 mM SDS obtained from the best computer fits. For experimental details, see Table II and the text.

Time-Resolved Fluorescence of M13 Coat Protein in Vesicles. The lifetimes and their preexponential factors in the range of 10–40 °C are listed in Table III. In Figure 4 the decay after excitation at 295 nm is shown. Similar values as given in Figure 4 were also found for the other L/P ratios from 20 to 410 at 20 °C (data not shown).

The fluorescence anisotropy in SUVs was fitted as a double exponential with a constant value $[r(\infty)]$. In Figure 5 the anisotropy decays of M13 coat protein in SUVs after excitation at 295 and 300 nm are shown. Table IV summarizes the results at various temperatures. The initial anisotropy, $r(0)$, is 0.16 after 295-nm and 0.23 after 300-nm excitation and in both cases independent of temperature (Table IV). The relative contribution of β_1 to the total anisotropy decay, i.e.,

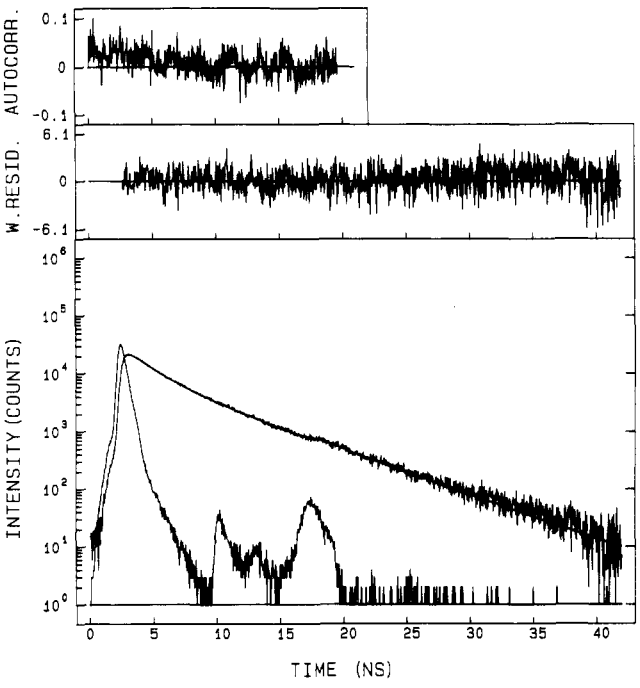

FIGURE 4: Fluorescence decay at 344 nm of the single tryptophan of bacteriophage M13 coat protein–DMPC/DMPA (80/20 w/w) SUVs of L/P ratio = 70 at 20 °C, the best computer fit, and the excitation pulse (295 nm). The parameters describing the best fit to the experimental decay and the estimated standard deviations are $\alpha_1 = 0.25 \pm 0.02$, $\alpha_2 = 0.44 \pm 0.02$, $\alpha_3 = 0.31 \pm 0.01$, $\tau_1 = 0.8 \pm 0.1$ ns, $\tau_2 = 2.2 \pm 0.1$ ns, and $\tau_3 = 5.5 \pm 0.1$ ns with the Durbin–Watson parameter = 1.82 and the number of zero passages = 202 (959 channels, 41 ps/channel). The weighted residuals from experimental and fitted curve and the autocorrelation function are given in the top of the figure.

$\beta_1/r(0)$, is 19% at 295-nm and 26% at 300 nm excitation. For other L/P ratios in the range of 20–410 at 20 °C, similar results are found (data not shown). The short correlation time, ϕ_1, was found to be nearly temperature independent (0.5 ± 0.2 ns). Therefore, ϕ_1 was fixed at 0.5 ns in the final computer fitting. The longer correlation time, ϕ_2, decreases at increasing temperature (Figure 6).

The order parameter S calculated from eq 4 is almost constant (0.7 ± 0.1) at all temperatures at 295– (Figure 6) and 300-nm excitation (Table IV).

Discussion

Micelles. In SDS micelles M13 coat protein forms a dimer (Tanford & Reynolds, 1976). The secondary structure of the coat protein in the SDS micelles is partly α-helix (60%) and partly β-structure (28%, Figure 1). This observation agrees with those previously reported (Nozaki et al., 1976, 1978; Chamberlain et al., 1978). Below the cmc (3 mM), the amount of β-structure increases to 64% at the expense of α-helix (16%). Under these conditions the coat protein is solubilized by SDS molecules. The higher amount of β-structure in the coat protein is probably due to the formation of larger aggregates as seen from the fluorescence anisotropy decay (to be discussed below). These aggregates could be similar to the coat protein polymer observed in vesicles in which also β-structure is dominant (94%), consistent with the work of Nozaki et al. (1978).

For all total fluorescence decays of the tryptophan in M13 coat protein, three lifetimes were required to obtain a satisfactory fit according to the criteria listed under Methods. This is in agreement with previously reported multiexponential decays for other single tryptophan proteins (Grinvald & Steinberg, 1976; Munro et al., 1979). The origin for this lies in the complex photophysics of the tryptophan residue, which is partly caused by the presence of different conformers (Szabo & Rayner, 1980; Chang et al., 1983; Petrich et al., 1983). We suggest that in a similar way in the M13 coat protein different conformers give rise to different lifetimes. These conformers arise from different average orientations of the tryptophan

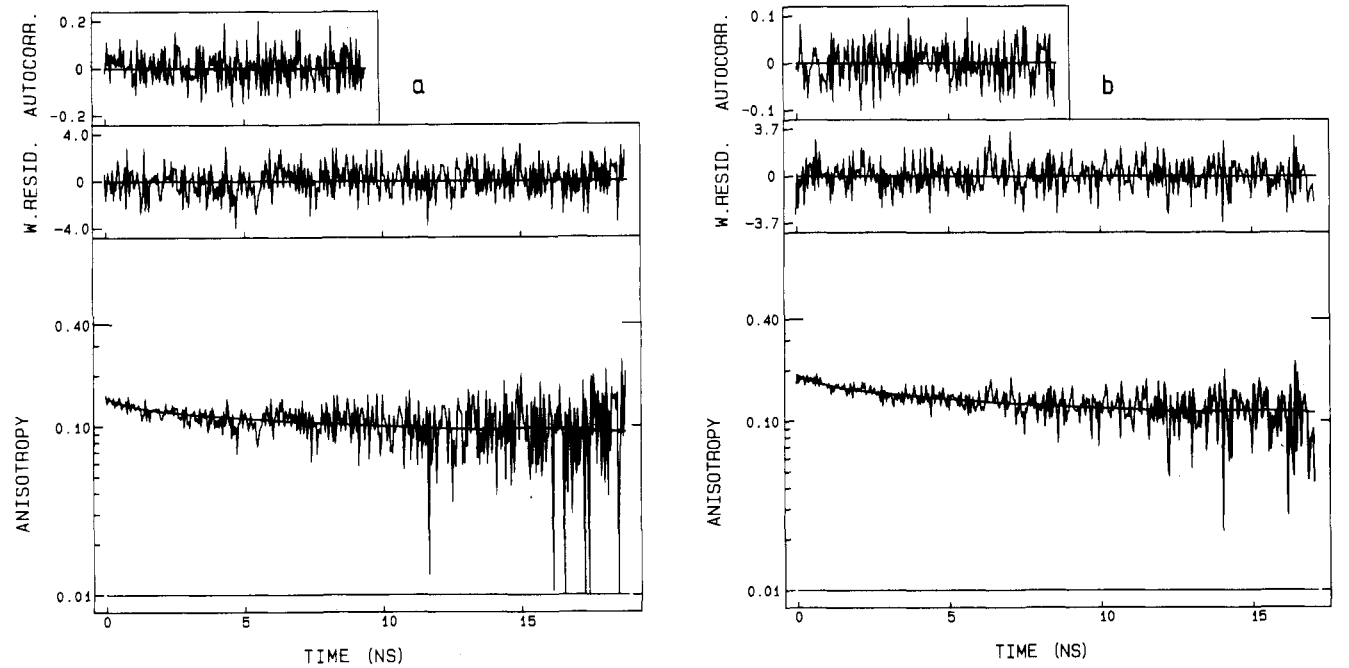

FIGURE 5: Anisotropy decays at 344 nm of the single tryptophan of bacteriophage M13 coat protein–DMPC/DMPA (80/20 w/w) SUVs of L/P ratio = 70 at 20 °C and the best computer fits after excitation at 295 (a) and 300 nm (b). The parameters describing the best fit to the experimental decay and the estimated standard deviations are (a) $\beta_1 = 0.03 \pm 0.006$, $\beta_2 = 0.04 \pm 0.006$, $r(\infty) = 0.09 \pm 0.007$, $\phi_1 = 0.5$ ns, and $\phi_2 = 8 \pm 2$ ns with the Durbin–Watson parameter = 1.87 and the number of zero passages in the parallel channel = 98 and in the perpendicular channel = 118 (460 channels, 41 ps/channel) and (b) $\beta_1 = 0.06 \pm 0.007$, $\beta_2 = 0.07 \pm 0.010$, $r(\infty) = 0.10 \pm 0.010$, $\phi_1 = 0.5$ ns, and $\phi_2 = 8 \pm 2$ ns with the Durbin–Watson parameter = 1.84 and the number of zero passages in the parallel channel = 84 and in the perpendicular channel = 97 (432 channels, 41 ps/channel). Only the initial parts of the anisotropy decays (of totally 1024 channels) are shown. The weighted residuals from the experimental and fitted curves and the autocorrelation functions are given in the top of the figures.

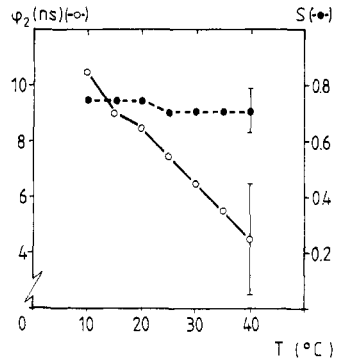

FIGURE 6: Temperature dependence of the longer correlation time, ϕ_2 (open circles), and order parameter, S (closed circles), of M13 coat protein in mixed SUVs of DMPC/DMPA (80/20 w/w) at L/P ratio of 70. For experimental details, see Table IV and the text.

indole ring with respect to the neighboring amide and carboxyl groups along the backbone of the coat protein.

Below the cmc, the fluorescence of the coat protein aggregate, solubilized by detergent molecules, is also triply exponential, but the lifetimes are significantly longer than those for the coat protein in micelles. However, α_2 increases at the expense of α_3. This indicates that in the solubilized coat protein conformation (64% β-structure as determined by CD, Figure 1) the quenching of the tryptophan fluorescence is more efficient, presumably due to changes in orientation of neighboring amide and carbonyl groups with respect to the indole ring.

The long-wavelength absorption band of the indole ring consists of two electronic transitions, ^1L_a and ^1L_b. The dipole moments of these transitions are almost perpendicular to each other. By excitation at 295 nm, both energy levels become populated (Weber, 1960; Valeur & Weber, 1977). Between these levels energy transfer can occur easily on a subnanosecond time scale (Cross et al., 1983). Nevertheless, it cannot be excluded that energy transfer between these two states provides an additional mechanism for the multiexponential decay of the fluorescence.

The fluorescence anisotropy is doubly exponential. The longer correlation time is assigned to the overall rotation of the coat protein–micelle complex for the following reasons. First, this correlation time is temperature dependent (Figure 3). The constancy of $RT\phi_2/\eta$ ($=V$, see Table II) indicates that the motion, which is characterized by ϕ_2, satisfies the Stokes–Einstein relation for isotropic rotational diffusion in solution. Second, below the cmc, i.e., under conditions in which coat protein is solubilized by detergent molecules and no micelles are formed, ϕ_2 increases as a result of the formation of larger coat protein–detergent aggregates. The average overall rotation of these complexes is therefore described by ϕ_2.

Above the cmc, the volume of the protein–micelle complex, V, can be used to obtain a rough estimate of the number of SDS molecules in these micelles, n. Using $V = 2M_p(v_p + h) + nM_{SDS}(v_{SDS} + h)$ in which v is the partial specific volume [$v_p = 0.74$ cm^3/g (Cantor & Schimmel, 1980); $v_{SDS} = 0.87$ cm^3/g (Tanford et al., 1974)] and h is the degree of hydration of the protein–micelle complex ($\sim$0.2 cm^3/g), it is calculated that n amounts to ca. 57. In this calculation two coat protein molecules per SDS micelle are assumed (Tanford & Reynolds, 1976). This value agrees very well with a previously determined ratio of 60 SDS molecules per coat protein dimer from independent measurements (Makino et al., 1975).

The shorter correlation time (0.5 ns) is independent of temperature and SDS concentration. This means that ϕ_1 characterizes a rapid, temperature-independent depolarization process within the coat protein. The mechanism, which is also present in the fluorescence anisotropy decay of coat protein in vesicles, will be discussed below.

Vesicles. In the samples of SUVs prepared by cholate dialysis, the protein is dominantly in β-structure conformation (Figure 1) independent of the L/P ratio. The β-structure has been observed before by CD of M13 coat protein in model membranes (Nozaki et al., 1976, 1978; Chamberlain et al., 1978). However, in the phage the structure is known to be entirely α-helix (Nozaki et al., 1976; Opella et al., 1987). This has been explained as a reflection of a major conformational change in the coat protein structure during the membrane-bound assembly of the phage (Nozaki et al., 1976).

For the triple-exponential fluorescence decay of tryptophan in M13 coat protein in vesicles, comparable lifetimes are found as in micelles, although the amplitude of the second lifetime, α_2, has increased significantly at the expense of α_3. This was also observed for solubilized coat protein in detergent solution below the cmc. The conformational change toward dominantly β-structure (94%, Figure 1) of M13 coat protein probably gives rise to a more efficient quenching process, determined by τ_2. The constancy of the fluorescence decay as a function of L/P ratio indicates that the coat protein conformation in vesicles that favors more efficient quenching is formed independently of L/P ratio. The fact that the fluorescence decays of coat protein in SUVs and detergent solution below the cmc are both dominated by τ_2 strongly suggests that the microenvironment of tryptophan is identical in both aggregation states of the coat protein.

The initial anisotropy, $r(0)$, of the coat protein in vesicles depends on the wavelength of excitation, 0.16 (295 nm) and 0.23 (300 nm), in agreement with previous measurements on other proteins (Lakowicz et al., 1983). From the initial and residual anisotropy, the order parameter of the tryptophan in the M13 coat protein is calculated to be 0.7 $\pm$ 0.1 (at 295- and 300-nm excitation) at all L/P ratios and temperatures measured. The fluorescence anisotropy does not decay to zero since the vesicle rotation is too slow on the nanosecond time scale to contribute to the decay, in contrast to the micellar rotation (ϕ_2 in Table II). The gel to liquid-crystalline phase transition of the lipid mixture DMPC/DMPA (80/20 w/w) was determined to be completed at 26 °C (unpublished results), which is 2 deg above the phase transition of pure DMPC. Thus, it appears from the fluorescence results that the M13 coat protein is not sensitive to the phase transition and the rapid motions of lipids in the liquid-crystalline phase. This suggests that the majority of the indole rings do not experience the lipid motion because of aggregation of the coat protein. The constancy of the order parameter is in agreement with deuterium NMR measurements of the amide sites along the M13 coat protein backbone in similar mixed bilayers, which show that the lipid motions do not affect the order of the amide deuterons along the coat protein backbone (K. P. Datema et al., unpublished results). For other single transmembrane proteins that do not aggregate, it has been found that the deuterium NMR order parameter reflects the gel to liquid-crystalline phase transition of the lipids (Pauls et al., 1985; Datema et al., 1986). For M13 coat protein it is therefore concluded that the protein in the bilayer is in an aggregated state. The concept of such protein aggregates is not in contradiction with the rigid protein structure proposed by Wolber and Hudson (1982).

Steady-state fluorescence studies of M13 coat protein in DMPC vesicles with parinaric acid have shown that the

fluorescence of the tryptophan of the coat protein is quenched by radiationless energy transfer to the probe lipid (Kimelman et al., 1979). Extensive protein–protein aggregation was excluded in that paper. This is not consistent with our findings. However, it should be noted that, in a protein aggregate, quenching is still possible by intertryptophan energy transfer and subsequent energy trapping by the lipid acceptor.

The correlation times ϕ_1 and ϕ_2 indicate an internal tryptophan flexibility within the coat protein aggregate. The larger correlation time, ϕ_2, is most likely related to segmental mobility of the coat protein within the aggregate. The shorter, temperature independent correlation time (0.5 ns) could arise from internal motion of the tryptophan indole ring but also from energy transfer from one indole ring to another in the aggregate, as demonstrated for aromatic dimers in solid solution (Visser et al., 1983).

In aggregated coat protein in the tryptophan rings are positioned close to each other, i.e., halfway along the peptide in the hydrophobic region. If ϕ_1 is caused by energy transfer between two nearby indole rings, then the contribution of β_1 would decrease if the excitation wavelength is shifted to the red edge of the light absorption spectrum (Weber, 1960; Weber & Shinitzky, 1970). On the other hand, in the case of rapid indole ring motion no such dependence is expected for β_1. Therefore, the anisotropy was measured also for 300-nm excitation. Since the relative contribution of β_1 increases if the excitation wavelength is changed from 295 to 300 nm, this observation suggests that ϕ_1 arises from rapid motion of the tryptophan ring in the coat protein.

Acknowledgments

We thank Dr. B. J. M. Harmsen for providing facilities to grow *E. coli* and K. Vos for an introduction to the software for fluorescence data analysis.

Registry No. DMPC, 18194-24-6; DMPA, 28874-52-4; SDS, 151-21-3.

References

Ameloot, M., & Hendrickx, H. (1982) *J. Chem. Phys. 76*, 4419–4432.

Bartlett, G. R. (1959) *J. Biol. Chem. 234*, 466–468.

Beechem, J. M., & Brand, L. (1985) *Annu. Rev. Biochem. 54*, 43–71.

Bevington, P. R. (1969) *Data Reduction and Error Analysis for the Physical Sciences*, McGraw-Hill, New York.

Cantor, C. R., & Schimmel, P. R. (1980) *Biophysical Chemistry*, Freeman, San Francisco.

Chamberlain, B. K., Nozaki, Y., Tanford, C., & Webster, R. E. (1978) *Biochim. Biophys. Acta 510*, 18–37.

Chang, M. C., Petrich, J. W., McDonald, D. B., & Fleming, G. R. (1983) *J. Am. Chem. Soc. 105*, 3819–3824.

Cross, A. J., & Fleming, G. R. (1984) *Biophys. J. 46*, 45–56.

Cross, A. J., Waldeck, D. H., & Fleming, G. R. (1983) *J. Chem. Phys. 78*, 6455–6467.

Cundall, R. B., & Dale, R. E., Eds. (1983) *Time-Resolved Fluorescence Spectroscopy in Biochemistry and Biology*, Plenum, New York.

Dale, R. E., Chen, L. A., & Brand, L. (1977) *J. Biol. Chem. 252*, 7500–7510.

Datema, K. P., Pauls, K. P., & Bloom, M. (1986) *Biochemistry 25*, 3796–3803.

Devaux, P. F., & Seigneuret, M. (1985) *Biochim. Biophys. Acta 822*, 63–125.

Garssen, G. J., Hilbers, C. W., Schoenmaker, J. G. G., & Van Boom, J. H. (1977) *Eur. J. Biochem. 81*, 453–463.

Geller, B. L., & Wickner, W. (1985) *J. Biol. Chem. 260*, 13281–13285.

Gilbert, C. W. (1983) in *Time-Resolved Fluorescence Spectroscopy in Biochemistry and Biology* (Cundall, R. B., & Dale, R. E., Eds.) pp 605–606, Plenum, New York.

Greenfield, N., & Fasman, G. D. (1969) *Biochemistry 8*, 4108–4116.

Grinvald, A., & Steinberg, I. Z. (1976) *Biochim. Biophys. Acta 427*, 663–678.

Hagen, D. S., Weiner, J. H., & Sykes, B. D. (1978) *Biochemistry 17*, 5860–5866.

Helenius, A., McCaslin, D. R., Fries, E., & Tanford, C. (1979) *Methods Enzymol. 63*, 734–749.

Hemminga, M. A. (1987) *J. Chem. Soc., Faraday Trans. 1, 83*, 203–209.

Hemminga, M. A., Datema, K. P., Ten Kortenaar, P. W. B., Krüse, J., Vriend, G., Verduin, B. J. M., & Koole, P. (1985) in *Magnetic Resonance in Biology and Medicine* (Govil, G., Khetrapal, C. L., & Saran, A., Eds.) pp 53–76, Tata McGraw-Hill, New Delhi, India.

Heyn, M. (1979) *FEBS Lett. 108*, 359–364.

Jaehnig, F. (1979) *Proc. Natl. Acad. Sci. U.S.A. 76*, 6361–6365.

Kimelman, D., Tecoma, E. S., Wolber, P. K., Hudson, B. S., Wickner, W., & Simoni, R. D. (1979) *Biochemistry 18*, 5874–5880.

Kinosita, K., Jr., Kawato, S., & Ikegami, A. (1977) *Biophys. J. 20*, 289–305.

Kinosita, K., Jr., Ikegami, A., & Kawato, S. (1982) *Biophys. J. 37*, 461–464.

Knippers, R., & Hoffmann-Berling, H. (1966) *J. Mol. Biol. 21*, 281–292.

Lakowicz, J. R., Maliwal, B. P., Cherek, H., & Balter, A. (1983) *Biochemistry 22*, 1741–1752.

Makino, S., Woolford, J. L., Jr., Tanford, C., & Webster, R. (1975) *J. Biol. Chem. 250*, 4327.

Marvin, D. A., & Wachtel, E. J. (1975) *Nature (London) 253*, 19–23.

Munro, I., Pecht, I., & Stryer, L. (1979) *Proc. Natl. Acad. Sci. U.S.A. 76*, 56–60.

Nakashima, Y., & Konigsberg, W. (1974) *J. Mol. Biol. 88*, 598–600.

Nozaki, Y., Chamberlain, B. K., Webster, R. E., & Tanford, C. (1976) *Nature (London) 259*, 335–337.

Nozaki, Y., Reynolds, J. A., & Tanford, C. (1978) *Biochemistry 17*, 1239–1246.

O'Connor, D. V., & Phillips, D. (1984) *Time-Correlated Single Photon Counting*, Academic, London.

Opella, S. J., Stewart, P. L., & Valentine, K. G. (1987) *Q. Rev. Biophys. 19*, 7–49.

Pauls, K. P., MacKay, A. L., Soederman, O., Bloom, M., Tanjea, A. K., & Hodges, R. S. (1985) *Eur. Biophys. J. 12*, 1–11.

Peterson, G. L. (1977) *Anal. Biochem. 83*, 346–356.

Petrich, J. W., Chang, M. C., McDonald, D. B., & Fleming, G. R. (1983) *J. Am. Chem. Soc. 105*, 3824–3832.

Szabo, A. (1984) *J. Chem. Phys. 81*, 150–167.

Szabo, A. G., & Rayner, D. M. (1980) *J. Am. Chem. Soc. 102*, 554–563.

Tanford, C., & Reynolds, J. A. (1976) *Biochim. Biophys. Acta 457*, 133–170.

Tanford, C., Nozaki, Y., Reynolds, J. A., & Makino, S. (1974) *Biochemistry 13*, 2369–2376.

Valeur, B., & Weber, G. (1977) *Photochem. Photobiol. 25*, 441–444.

Van Asbeck, F., Beyreuther, K., Koehler, H., Von Wettstein, G., & Braunitzer, G. (1969) *Hoppe-Seyler's Z. Physiol. Chem. 350*, 1047-1066.
Van der Meer, W., Pottel, H., Herreman, W., Ameloot, M., Hendrickx, H., & Schroeder, H. (1984) *Biophys. J. 46*, 515-523.
Van Hoek, A., & Visser, A. J. W. G. (1985) *Anal. Instrum. (N.Y.) 14*, 359-378.
Van Hoek, A., Vervoort, J., & Visser, A. J. W. G. (1983) *J. Biochem. Biophys. Methods 7*, 243-254.
Visser, A. J. W. G., Santema, J. S., & Van Hoek, A. (1983) *Photobiochem. Photobiophys. 6*, 47-55.
Visser, A. J. W. G., Ykema, T., Van Hoek, A., O'Kane, D. J., & Lee, J. (1985) *Biochemistry 24*, 1489-1496.
Vos, K., Van Hoek, A., & Visser, A. J. W. G. (1987) *Eur. J. Biochem. 165*, 55-63.
Watts, A., & Depont, J. J. H. H. M., Eds. (1985) *Progress in Protein-Lipid Interactions*, Elsevier, New York.
Weber, G. (1960) *Biochem. J. 75*, 335-345.
Weber, G., & Shinitzky, M. (1970) *Proc. Natl. Acad. Sci. U.S.A. 65*, 823-830.
Wickner, W. (1976) *Proc. Natl. Acad. Sci. U.S.A. 73*, 1159-1163.
Wolber, P. K., & Hudson, B. S. (1982) *Biophys. J. 37*, 253-262.
Zannoni, C., Arcioni, A., & Cavatorta, P. (1983) *Chem. Phys. Lipids 32*, 179-250.

Reactivity of Chemically Cross-Linked Fibrinogen and Its Fragments D toward the Staphylococcal Clumping Receptor†

Marek Kloczewiak, Sheila Timmons, and Jacek Hawiger*

Division of Experimental Medicine, Department of Medicine, New England Deaconess Hospital and Harvard Medical School, Boston, Massachusetts 02215

Received December 5, 1986; Revised Manuscript Received April 15, 1987

ABSTRACT: It has been established that the binding domain for the staphylococcal clumping receptor exists in fragment D of human fibrinogen [Hawiger J., Timmons, S., Strong, D. D., Cottrell, B. A., Riley, M., & Doolittle, R. F. (1982) *Biochemistry 21*, 1407; Strong, D. D., Laudano, A., Hawiger, J., & Doolittle, R. F. (1982) *Biochemistry 21*, 1414]. To examine the role of valency in the adhesive function of fibrinogen, its fragments were prepared by digestion with plasmin in the presence of calcium and purified by a two-step chromatographic procedure. Fragments D_1 and E did not induce the staphylococcal clumping reaction. After they were prepared in oligomeric form by chemical cross-linking with glutaraldehyde, fragment D_1 (M_r 94 000) became functionally reactive toward the staphylococcal clumping receptor, and fragment D_3 (M_r 75 000) and fragment E (M_r 50 000) remained inactive. Fragment D dimer derived from enzymatic cross-linking was not reactive. Human fibrinogen cross-linked with glutaraldehyde usually reached a 250 times higher reactivity toward the staphylococcal clumping receptor, depending on the condition of the cross-linking reaction. It is concluded that the valency of fibrinogen in regard to its receptor binding domain and the availability of this domain are essential for the staphylococcal clumping reaction.

Fibrinogen, which has a dimeric structure, is able to cross-bridge receptors present on individual staphylococci or platelets, forming visible aggregates of these cells (Hawiger et al., 1982a,b; Strong et al., 1982; Kloczewiak et al., 1984). Although a plasmin degradation product of fibrinogen, fragment D_1,[1] still binds to staphylococci and inhibits the binding and the clumping reaction of intact fibrinogen, no staphylococcal clumping reaction could be elicited by fragment D_1 (Hawiger et al., 1982a). To test the hypothesis that the cell agglutinating property of fibrinogen toward staphylococci was dependent on the dimeric structure of fibrinogen, we isolated monovalent fibrinogen fragments D_1 and D_3 which possess or lack, respectively, the binding domain for the staphylococcal clumping receptor (Hawiger et al., 1982a; Strong et al., 1982). The 15-residue carboxy-terminal segment of the γ-chain that interacts with the staphylococcal clumping receptor also bears sites for enzymatic cross-linking by factor XIIIa (Chen & Doolittle, 1970; Strong et al., 1982). Therefore, we compared chemically cross-linked D_1 oligomers with enzymatically cross-linked fragment D (D dimer) to see whether factor XIIIa induced cross-links interfere with receptor recognition of the

† This work was supported by Research Grants HL-30647, HL-33014, and HL-35437 from the National Institutes of Health, U.S. Public Health Service.

[1] Abbreviations: CU, casein unit(s); TIU, trypsin inhibitor unit(s); Tris-HCl, 2-amino-2-(hydroxymethyl)-1,3-propanediol hydrochloride; CM, carboxymethyl; DEAE, diethylaminoethyl; $NaDodSO_4$, sodium dodecyl sulfate; EDTA, ethylenediaminetetraacetic acid; dansyl, 5-(dimethylamino)naphthalene-1-sulfonyl; PPACK, D-phenylalanyl-L-propyl-L-arginine chloromethyl ketone; $NaBH_4$, sodium borohydride. Fragments obtained by plasmic degradation of fibrinogen are denoted as follows: D_1 is a 94-kDa fragment from the carboxy-terminal domain encompassing chain remnants α105-206, β134-461, and γ63-411; D_3 is a 75-kDa fragment derived from D_1 by proteolytic removal of the carboxy terminal of the γ-chain resulting in the remnant γ63-302; D dimer is an enzymatically cross-linked fragment D via ϵ-(γ-glutamyl)lysyl isopeptide bonds between the carboxy-terminal regions of the two γ-chain remnants; E is a 50-kDa fragment derived from the central, amino-terminal domain of fibrinogen and encompassing chain remnants α24-78, β54-120, and γ1-53.

0006-2960/87/0426-6152$01.50/0